Elliptic Flow: Transition from Out-of-Plane to In-Plane Emission in Au + Au Collisions

C. Pinkenburg,[1] N. N. Ajitanand,[1] J. M. Alexander,[1] M. Anderson,[5] D. Best,[2] F. P. Brady,[5] T. Case,[2] W. Caskey,[5] D. Cebra,[5] J. L. Chance,[5] P. Chung,[1] B. Cole,[12] K. Crowe,[2] A. C. Das,[3] J. E. Draper,[5] A. Elmaani,[1] M. L. Gilkes,[1] S. Gushue,[1,9] M. Heffner,[5] A. S. Hirsch,[7] E. L. Hjort,[7] L. Huo,[14] M. Justice,[4] M. Kaplan,[8] D. Keane,[4] J. C. Kintner,[13] J. Klay,[5] D. Krofcheck,[11] R. A. Lacey,[1] J. Lauret,[1] C. Law,[1] M. A. Lisa,[3] H. Liu,[4] Y. M. Liu,[14] R. McGrath,[1] Z. Milosevich,[8] G. Odyniec,[2] D. L. Olson,[2] S. Y. Panitkin,[4] N. T. Porile,[7] G. Rai,[2] H. G. Ritter,[2] J. L. Romero,[5] R. Scharenberg,[7] L. Schroeder,[2] B. Srivastava,[7] N. T. B Stone,[2] T. J. M. Symons,[2] J. Whitfield,[8] T. Wienold,[2] R. Witt,[4] L. Wood,[5] and W. N. Zhang[14]

(E895 Collaboration)

P. Danielewicz[6] and P. B. Gossiaux[10]

[1]*Departments of Chemistry and Physics, State University of New York, Stony Brook, New York 11794*
[2]*Lawrence Berkeley National Laboratory, Berkeley, California 94720*
[3]*Ohio State University, Columbus, Ohio 43210*
[4]*Kent State University, Kent, Ohio 44242*
[5]*University of California, Davis, California 95616*
[6]*Michigan State University, East Lansing, Michigan 48824-1321*
[7]*Purdue University, West Lafayette, Indiana 47907-1396*
[8]*Carnegie Mellon University, Pittsburgh, Pennsylvania 15213*
[9]*Brookhaven National Laboratory, Upton, New York 11973*
[10]*SUBATECH, Ecole des Mines, F-44070 Nantes, France*
[11]*University of Auckland, Auckland, New Zealand*
[12]*Columbia University, New York, New York 10027*
[13]*St. Mary's College, Moraga, California 94575*
[14]*Harbin Institute of Technology, Harbin, 150001 People's Republic of China*

(Received 21 September 1998)

We have measured the proton elliptic flow excitation function for the Au + Au system spanning the beam energy range $(2-8)A$ GeV. The excitation function shows a transition from negative to positive elliptic flow at a beam energy, $E_{\mathrm{tr}} \sim 4A$ GeV. Detailed comparisons with calculations from a relativistic Boltzmann equation are presented. The comparisons suggest a softening of the nuclear equation of state from a stiff form ($K \sim 380$ MeV) at low beam energies ($E_{\mathrm{beam}} \leq 2A$ GeV) to a softer form ($K \sim 210$ MeV) at higher energies ($E_{\mathrm{beam}} \geq 4A$ GeV) where the calculated baryon density $\rho \sim 4\rho_0$.

PACS numbers: 25.75.Ld, 21.65.+f, 24.10.Jv

For many years, the investigation of the nuclear equation of state (EOS) has stood out as one of the primary driving forces for heavy ion reaction studies (e.g., [1,2]). Measurements of collective motion and, in particular, the elliptic flow have been predicted to provide information crucial for establishing the parameters of the EOS [3–5]. Theoretical conjectures have also focused on the notion that a transition to the quark-gluon plasma (QGP) is associated with a "softest point" in the EOS where the pressure increase with temperature is much slower than the energy density [6]. Such a softening of the EOS is predicted to start at quark-antiquark densities comparable to those in the ground state of nuclear matter [7], and also at relatively low temperatures if the baryon density is driven significantly beyond its normal value ρ_0 [8,9]. At energies of $1A \lesssim E_{\mathrm{beam}} \lesssim 11A$ GeV, collision-zone matter densities are expected up to $\rho \sim (6-8)\rho_0$ [8,10]. Such densities could very well result in conditions favorable to a softening of the EOS. Therefore, it is important to investigate currently available elliptic flow data [in this energy range] to search for new insights into the parameters of the EOS and for any indication of its softening.

Elliptic flow reflects the anisotropy of transverse particle emission at midrapidity. For beam energies of $(1-11)A$ GeV this anisotropy results from a strong competition between "squeeze-out" and "in-plane flow" [3,5,8]. The magnitude and the sign of elliptic flow depend on two factors: (i) the pressure built up in the compression stage compared to the energy density, and (ii) the passage time of the projectile and target spectators. The characteristic time for the development of expansion perpendicular to the reaction plane can be estimated as $\sim R/c_s$, where the speed of sound $c_s = \sqrt{\partial p/\partial e}$, R is the nuclear radius, p is the pressure, and e is the energy density. The passage time is $\sim 2R/(\gamma_0 v_0)$, where v_0 is the cm spectator velocity. Thus the squeeze-out contribution

should reflect the ratio $c_s/\gamma_0 v_0$ [4] which is responsible for the essentially logarithmic dependence of elliptic flow on the beam energy for $\sim 1A \leq E_{\text{beam}} \leq 11A$ GeV [8].

Recent calculations have made specific predictions for the beam energy dependence of elliptic flow for Au + Au collisions at $(1-11)A$ GeV [8]. They indicate a transition from negative to positive elliptic flow at a beam energy E_{tr}, which has a marked sensitivity to the stiffness of the EOS. In addition, they suggest that a phase transition to the QGP should give a characteristic signature in the elliptic flow excitation function due to significant softening of the EOS. In this Letter we present an experimental elliptic flow excitation function for the Au + Au system to establish E_{tr} and to search for any hints of a softening of the EOS.

The measurements were performed at the Alternating Gradient Synchrotron at the Brookhaven National Laboratory. Beams of ^{197}Au ($E_{\text{beam}} = 2A$, $4A$, $6A$, and $8A$ GeV) [11] were used to bombard a ^{197}Au target of thickness calculated for a 3% interaction probability. Typical beam intensities resulted in ~ 10 spills/min with $\sim 10^3$ particles per spill. Charged reaction products were detected with the E895 experimental setup which consists of a time projection chamber (TPC) [12] and a multisampling ionization chamber (MUSIC) [13]. The TPC which was located in a magnet (typically at 1.0 T) provided good acceptance and charge resolution for charged particles $-1 < Z < 6$ at all four beam energies. However, unique mass resolution for $Z = 1$ particles was not achieved for all rigidities. The MUSIC device, positioned ~ 10 m downstream of the TPC, provided unique charge resolution for fragments with $Z > 7$ for the $2A$ and $4A$ GeV beams. Data were taken with a trigger for minimum bias and also for a bias toward central and midcentral collisions. Results are presented here for protons measured in the TPC for midcentral collisions.

We use the second Fourier coefficient $v_2 = \langle \cos 2\phi \rangle$, to measure the elliptic flow or azimuthal asymmetry of the proton distributions at midrapidity ($|y_{\text{cm}}| < 0.1$) ;

$$\frac{dN}{d\phi} \sim [1 + 2v_1 \cos(\phi) + 2v_2 \cos(2\phi)]. \qquad (1)$$

Here, ϕ represents the azimuthal angle of an emitted proton relative to the reaction plane. The Fourier coefficient $\langle \cos 2\phi \rangle = 0$, >0, and <0 for zero, positive, and negative elliptic flow, respectively. Measurements of v_1 will be presented and discussed in a forthcoming paper [14].

Our analysis proceeds in two steps. First, we determine the reaction plane and its associated dispersion for each beam energy. Second, we generate azimuthal distributions with respect to this experimentally determined reaction plane and evaluate $\langle \cos 2\phi \rangle$. The vector $\mathbf{Q}_i = \sum_{j \neq i}^{n} w(y_j) \mathbf{p}_j^t / p_j^t$ is used to determine the azimuthal angle, Φ_{plane}, of the reaction plane [15]. Here, $\mathbf{p}_j^t$ and y_j represent, respectively, the transverse momentum and the rapidity of baryon j ($Z \leq 2$) in an event. The weight $w(y_j)$ is assigned the value $\frac{\langle p^x \rangle}{\langle p^t \rangle}$, where p^x is the transverse momentum in the reaction plane. $\langle p^x \rangle$ is obtained from the first pass of an iterative procedure.

The dispersion of the reaction plane as well as biases associated with detector efficiencies plays a central role in flow analyses [16–18]. Consequently, in Fig. 1 we show representative distributions for the experimentally determined reaction plane (Φ_{plane}), and the associated relative reaction-plane distributions (Φ_{12}). The distributions have been generated for a midcentral impact parameter, i.e., multiplicities between 0.5 and $0.75 M_{\text{max}}$. Here, M_{max} is the multiplicity corresponding to the point in the charged particle multiplicity distribution where the height of the multiplicity distribution has fallen to half its plateau value [19]. It is estimated that this multiplicity range corresponds to an impact parameter range $\sim 5-7$ fm. The Φ_{12} distributions (cf. Fig. 1) which are important for assessing the role of the reaction-plane dispersion, have been obtained via the subevent method [15]. That is, reaction planes were determined for two subevents constructed from each event; Φ_{12} is the absolute value of the relative azimuthal angle between these two estimated reaction planes. The essentially flat reaction plane distributions shown in Fig. 1a reflect rapidity and multiplicity-dependent azimuthal efficiency corrections, applied to take account of the detection inefficiencies of the TPC. These corrections were obtained by accumulating the laboratory azimuthal distribution of the particles (as a function of rapidity and multiplicity) for all events and then including the inverse of these distributions in the weights for the determination of the reaction plane. The distributions shown in Fig. 1a confirm the absence of significant distortions which could influence the magnitude of the extracted elliptic flow. The relative reaction-plane distributions (Φ_{12}) shown in Fig. 1b indicate mean values which increase with the beam energy from $\langle \Phi_{12} \rangle / 2 \sim 17.0°$ at $2A$ GeV to $\sim 36.1°$ at $8A$ GeV. This increase suggests a progressive deterioration in the resolution of the reaction plane with increasing beam energy; however, a reasonable

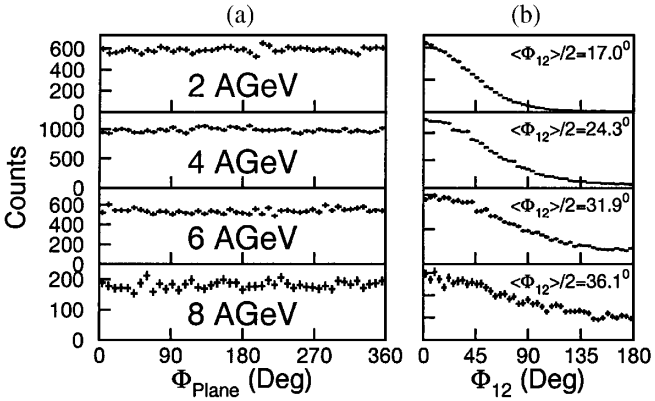

FIG. 1. Experimentally determined (a) reaction-plane (Φ_{plane}) distributions, and (b) the associated relative reaction-plane distributions (Φ_{12}) for $2A$, $4A$, $6A$, and $8A$ GeV Au + Au. The reaction plane distributions include efficiency corrections for the TPC (see text).

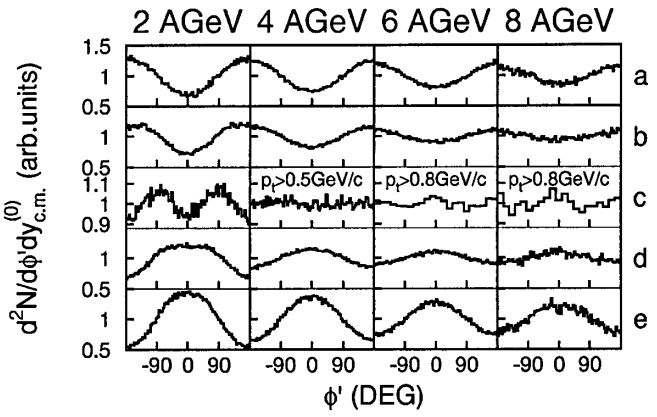

FIG. 2. Azimuthal distributions (with respect to the reconstructed reaction plane) for 2*A*, 4*A*, 6*A*, and 8*A* GeV Au + Au. Distributions are for (a) $-0.7 < y_{\rm cm} < -0.5$, (b) $-0.5 < y_{\rm cm} < -0.3$, (c) $-0.1 < y_{\rm cm} < 0.1$, (d) $0.3 < y_{\rm cm} < 0.5$, and (e) $0.5 < y_{\rm cm} < 0.7$. The midrapidity selections for (4–8)*A* GeV include a transverse momentum selection as indicated.

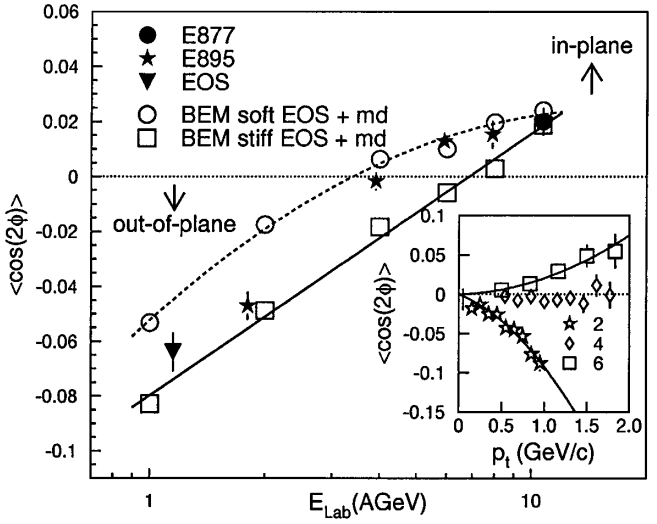

FIG. 3. Elliptic flow excitation function for Au + Au. The filled symbols represent the experimental data as indicated. The dashed curve (open circles) and the solid curve (open squares) represent the calculated excitation functions for a soft and a stiff EOS (momentum dependent), respectively. The inset shows the (dispersion corrected) transverse momentum dependence of the elliptic flow for the 2*A*, 4*A*, and 6*A* GeV beams.

resolution is maintained over the entire energy range. The Φ_{12} distributions serve as the basis for correcting the extracted elliptic flow values as discussed below.

In Fig. 2, we show observed (or ϕ') azimuthal distributions, for protons. These distributions, for several rapidities, have been generated for the same impact parameter range (~5–7 fm) discussed above. Several characteristic features are exhibited in Fig. 2. For example, as one moves away from midrapidity, the ϕ' distributions exhibit shapes commonly attributed to collective sidewards flow. That is, for $y > 0$, the distributions peak at 0°, and, for $y < 0$, they peak at ±180°. Figure 2 also shows that these anisotropies decrease with increasing beam energy.

The primary feature of the midrapidity distributions contrasts with those at other rapidities. At 2*A* GeV, two distinct peaks can be seen at −90° and +90°. These peaks indicate a clear signature for squeeze-out perpendicular to the reaction plane [16,19–22] or negative elliptic flow. By contrast, at 6*A* GeV and 8*A* GeV, the midrapidity distributions peak at 0° and ±180°. This latter anisotropy pattern is expected for positive elliptic flow. Thus, Fig. 2c provides clear evidence for negative elliptic flow at 2*A* GeV, positive elliptic flow for 6*A* and 8*A* GeV, and near zero flow for $E_{\rm beam} = 4$ GeV.

In order to quantify the proton elliptic flow, it is necessary to suppress possible distortions from imperfect particle identification (PId). It is relevant to reiterate that unique separation of π^+ and protons was not achieved for all rigidities. To suppress such ambiguity we applied the following procedure. First, we plot the observed Fourier coefficient $\langle \cos 2\phi' \rangle$ vs p_t with p_t thresholds which allow clean particle separation ($p_t \sim 1$ GeV/c). We then extract the coefficients for the quadratic dependence of $\langle \cos 2\phi' \rangle$ on p_t (see inset in Fig. 3). These quadratic fits are restricted by the requirement that $\langle \cos 2\phi' \rangle = 0$ for $p_t = 0$. Second, we correct the proton p_t distributions for possible π^+ contamination by way of a probabilistic PId. The probabilities were obtained by extrapolating the exponential tails of the proton and π^+ rigidity distributions into the regions of overlap. A weighted average (relative number of protons in a p_t bin times the $\langle \cos 2\phi' \rangle$ for that bin) was then performed to obtain $\langle \cos 2\phi' \rangle$ for each beam energy. Subsequent to this evaluation, we used the relative reaction plane distribution at each beam energy (cf. Fig. 1) to obtain dispersion corrections for the extracted Fourier coefficients [15,17,21].

The relationship between the $\langle \cos 2\phi' \rangle$ (obtained with the estimated reaction plane) and the Fourier coefficient $\langle \cos 2\phi \rangle$ relative to the true reaction plane is

$$\langle \cos 2\phi' \rangle = \langle \cos 2\phi \rangle \langle \cos 2\Delta\Phi \rangle , \qquad (2)$$

where $\langle \cos 2\Delta\Phi \rangle$ is the correction factor determined from the $\langle \cos \Phi_{12} \rangle$ [17]. Following the prescription outlined in Ref. [17], we find correction factors which range from 0.79 at 2*A* GeV to 0.29 at 8*A* GeV. The correction factors are summarized along with ($\langle \cos \Phi_{12} \rangle$) in Table I.

The corrected elliptic flow values, $\langle \cos 2\phi \rangle$, are represented by filled stars in Fig. 3. This excitation function clearly shows an evolution from negative to positive elliptic flow within the region $2A \lesssim E_{\rm beam} \lesssim 8A$ GeV and points to an apparent transition energy $E_{\rm tr} \sim 4A$ GeV. The solid and dashed curves represent the results of model

TABLE I. Dispersion correction factors for each beam energy.

Beam Energy (*A* GeV)	$\langle \cos \Delta\Phi_{12} \rangle$	$\langle \cos 2(\Delta\Phi) \rangle$
2	0.753	0.79
4	0.563	0.62
6	0.359	0.42
8	0.244	0.29

calculations described below. Since the value of $E_{\rm tr}$ is predicted to be sensitive to the parameters of the EOS [8], it is important to examine additional constraints on its value. The inset of Fig. 3 shows the corrected $\langle \cos 2\phi \rangle$ values as a function of p_t for protons. The solid curves in the figure represent quadratic fits to the data (2A and 6A GeV) which are in agreement with the predicted quadratic dependence of $\langle \cos 2\phi \rangle$ on p_t [4,20]. Of greater significance is the fact that a comparison of the p_t dependence of the elliptic flow, for 2A, 4A, and 6A GeV, provides further direct evidence that the sign of elliptic flow changes as the beam energy is increased from 2A to 6A GeV. The essentially flat p_t dependence shown for 4A GeV is consistent with $E_{\rm tr} \sim 4A$ GeV.

To interpret these data, extensive calculations were made to constrain parameters of the EOS in the context of a newly developed relativistic Boltzmann-equation model [8,23]. The phenomenological relativistic Landau theory of quasiparticles [24] serves as a basis for the model which has nucleon, pion, Δ, and N^* resonance degrees of freedom as well as momentum dependent forces. Calculations were performed for both a soft ($K = 210$ MeV), and a stiff ($K = 380$ MeV) EOS for the same rapidity and impact parameter selections applied to the data.

The elliptic flow excitation functions [25] are compared to the experimental data in Fig. 3. The dashed curve (open circles) represents the results for a soft EOS and the solid curve (open squares) represents results for a stiff EOS. In addition to the data from the present experiment (filled stars), Fig. 3 also shows experimental results for Au + Au reactions at 1.15A GeV [26] (filled triangle) and 10.8A GeV [27] (filled circle). The experimental data are compatible with the excitation function predicted for a stiff EOS at beam energies $1A \lesssim E_{\rm beam} \leq 2A$ GeV. By contrast, the data show good agreement with the predictions for a soft EOS for $4A \leq E_{\rm beam} \lesssim 11A$ GeV. This pattern is consistent with a softening of the EOS in semicentral collisions of Au + Au at $\sim$4A GeV. The calculated densities at maximum compression for these energies are of the order of $\sim 4\,\rho_0$ for the stiff EOS.

In summary, we have measured an elliptic flow excitation function for midcentral collisions of Au + Au at 2A, 4A, 6A, and 8A GeV. The excitation function exhibits a transition from negative to positive elliptic flow with $E_{\rm tr} \sim 4A$ GeV. Detailed comparisons of these elliptic flow data have been made with calculated results from a relativistic Boltzmann-equation calculation. Within the context of a simple parametrization of the EOS, the calculations suggest an evolution from a stiff EOS ($K \sim 380$ MeV) at low beam energies ($\leq$2A GeV) to a softer EOS ($K \sim 210$ MeV) at higher beam energies ($4A \leq E_{\rm beam} \lesssim 11A$ GeV). Such a softening of the EOS could result from a number of effects, the most intriguing of which is the possible onset of a nuclear phase change [8]. On the other hand, it should be noted that transport models have failed to reproduce low energy squeeze-out data with a single incompressibility constant [22]. Thus, additional experimental signatures as well as calculations based on other models will be necessary to test the detailed implications of these results. Nevertheless, the results presented here clearly show that elliptic flow measurements can provide an important constraint on the EOS of high density nuclear matter.

This work was supported in part by the U.S. Department of Energy under Grants No. DE-FG02-87ER40331.A008, No. DE-FG02-89ER40531, No. DE-FG02-88ER40408, No. DE-FG02-87ER40324, and Contract No. DE-AC03-76SF00098; by the U.S. National Science Foundation under Grants No. PHY-98-04672, No. PHY-9722653, No. PHY-96-05207, No. PHY-9601271, and No. PHY-9225096; and by the University of Auckland Research Committee, NZ/USA Cooperative Science Programme CSP 95/33.

[1] H. Stocker and W. Greiner, Phys. Rep. **137**, 277 (1986).
[2] *Quark Matter '96, Proceedings of the 12th International Conference on Ultra-Relativistic Nucleus-Nucleus Collisions, Heidelberg, Germany, 1996,* edited by P. Braun-Munzinger *et al.* [Nucl. Phys. **A610**, 1c–572c (1996)].
[3] J.-Y. Ollitrault, Phys. Rev. D **46**, 229 (1992).
[4] P. Danielewicz, Phys. Rev. C **51**, 716 (1995).
[5] H. Sorge, Phys. Rev. Lett. **78**, 2309 (1997).
[6] C. M. Hung and E. V. Shuryak, Phys. Rev. Lett. **75**, 4003 (1995).
[7] E. Laermann, in Ref. [2], p. 1c.
[8] P. Danielewicz *et al.*, Phys. Rev. Lett. **81**, 2438 (1998).
[9] G. Baym and S. A. Chin, Phys. Lett. **62B**, 241 (1976).
[10] B. A. Li and C. M. Ko, Nucl. Phys. **A601**, 457 (1996).
[11] After correction for energy loss in the beam line and the target, the respective energies are 1.8A, 3.9A, 5.9A, and 7.9A GeV.
[12] G. Rai *et al.*, IEEE Trans. Nucl. Sci. **37**, 56 (1990).
[13] G. Bauer *et al.*, Nucl. Instrum. Methods Phys. Res., Sect. A **386**, 249 (1997).
[14] E895 Collaboration, H. Liu *et al.* (to be published).
[15] P. Danielewicz and G. Odyniec, Phys. Lett. **157B**, 146 (1985).
[16] P. Danielewicz *et al.*, Phys. Rev. C **38**, 120 (1988).
[17] J.-Y. Ollitrault, Nucl. Phys. **A638**, 195c (1998); nucl-ex/9711003.
[18] A. M. Poskanzer and S. A. Voloshin, Phys. Rev. C **58**, 1671 (1998).
[19] H. H. Gutbrod *et al.*, Phys. Lett. B **216**, 267 (1989).
[20] D. Brill *et al.*, Z. Phys. A **355**, 61 (1996).
[21] M. Demoulins *et al.*, Phys. Lett. B **241**, 476 (1990).
[22] S. Wang *et al.*, Phys. Rev. Lett. **76**, 3911 (1996).
[23] P.-B. Gossiaux, *Advances in Nuclear Dynamics 4,* edited by W. Bauer and H. G. Ritter (Plenum, New York, 1998).
[24] G. Baym and S. A. Chin, Nucl. Phys. **A262**, 527 (1976).
[25] Calculations without composite particle production.
[26] EOS Collaboration, M. Partlan *et al.* (to be published).
[27] P. Braun-Munzinger and J. Stachel, Nucl. Phys. **A638**, 3c (1998), and references therein.